Simple interpretation of proton-neutron interactions in rare earth nuclei

Y. Oktem,[1,*] R. B. Cakirli,[1,2] R. F. Casten,[2,3] R. J. Casperson,[2] and D. S. Brenner[4]
[1]*Department of Physics, Istanbul University, Turkey*
[2]*Wright Nuclear Structure Laboratory, Yale University, New Haven, Connecticut 06520, USA*
[3]*Institut für Kernphysik, Universität zu Köln, Köln, Germany*
[4]*Department of Chemistry, Clark University, Worcester, Massachusetts 01610, USA*
(Received 8 June 2006; published 25 August 2006)

The rare earth nuclei from $N = 92$ to $N = 108$ display a very regular pattern of empirically extracted interactions of the last protons with the last neutrons. The simplicity of the empirical systematics suggests that a simple interpretation should be possible. We discuss calculations of these proton-neutron (p-n) interactions with a zero-range δ force.

DOI: 10.1103/PhysRevC.74.027304 PACS number(s): 21.30.Fe, 21.10.Dr, 21.60.Ev, 27.60.+j

It is possible to extract empirical values of the average interactions of the last two protons with the last two neutrons, called δV_{pn}, from double differences of binding energies. This was first suggested [1] and carried out [2–4] about fifteen years ago based on the masses then available. The recent 2003 mass evaluation [5] has expanded the number of available masses considerably and has led to recent studies of these interactions [6–8]. These studies focused on the striking behavior across major shell gaps [6] and the relation of the proton-neutron (p-n) interaction strengths to the growth of collectivity and deformation in particle-particle (p-p), particle-hole (p-h), and hole-hole (h-h) regions [7]. In Ref. [8], a global summary of all δV_{pn} values was presented. A number of patterns as well as anomalies were identified, but perhaps the most striking feature was a remarkable regularity in the mass region $A \sim 150$–180. The relevant δV_{pn} values are shown in Fig. 1.

The behavior is indeed striking. For each element these valence p-n interaction strengths grow systematically and substantially with N. The values for each successive Z are shifted systematically to the right, giving nearly perfect parallel trajectories. For those elements where sufficient data are known, a falloff at the largest neutron numbers is also observed. Behavior as regular and simple as this suggests that there must be a simple underlying microscopic physics interpretation. Previous investigations of δV_{pn} values [6–8] have focused on simple arguments relating to the spatial overlaps of proton and neutron orbits [9]. For example, near ^{208}Pb stronger interactions were found [6] for nuclei where both protons and neutrons were above shell closures, or where both were below, than when protons were above $Z = 82$ and neutrons below $N = 126$. The reason is simply the generic behavior of shell structure in heavy nuclei in which the normal parity orbits have typical sequences of nlj values ranging from low n high j to high n low j. This was also the explanation for the empirically noted higher growth rates of collectivity in p-p and h-h regions (each filling similar orbits) compared with p-h regions [7].

It would seem likely that a similar explanation should apply in the present case. Indeed, it was speculated in Ref. [8] that the systematic behavior of Nilsson orbits (these are all deformed nuclei) from equatorial (low Ω) to polar (high Ω) provides an explanation. The relevant proton numbers $Z = 64-74$ are near or above mid-shell and are therefore flat or slightly upsloping in the Nilsson scheme. The neutrons, however, are filling from $N = 92$ to around mid-shell. Hence, for a given Z, the p-n overlap of the last neutrons with the last protons should increase with N as more similar orbits are occupied.

It is the purpose of this Brief Report to focus on the systematics in Fig. 1 and on calculations, using a zero-range δ interaction, including spin exchange, of p-n interaction matrix elements to test whether these simple ideas are validated and whether the data plotted in Fig. 1 can be reproduced.

We consider the interaction of the last proton with the last neutron, both occupying Nilsson orbits. To do so, we use the standard expression of a Nilsson wave function in a spherical basis:

$$\Psi^{(\Omega)}_{\text{Nils}} = \sum_j C^{\Omega}_j \Phi^{(\Omega)}_{j(\text{sph})}. \tag{1}$$

The nuclei of interest, those in Fig. 1 with neutron numbers from $N = 92$ to $N = 108$, are all well deformed with deformation $\epsilon_2 \sim 0.3$. In this deformation range the C_j coefficients [10] are weakly dependent on ϵ_2, and so we use a single set of Nilsson wave functions (test calculations of the resulting p-n interactions show virtually no dependence on ϵ_2 in the range 0.2–0.3). The interaction matrix elements, $\langle \Omega^p, \Omega^n | V_{pn} | \Omega^p, \Omega^n \rangle$, where we have simplified the Nilsson notation $\Omega\,[Nn_z\Lambda]$ to Ω, are given by a sum over the matrix elements for the four cases of Ω_p, Ω_n both positive, both negative, or one of each sign. For example, for the case of $\Omega^{\text{tot}} = \Omega^p + \Omega^n$, we have

$$\begin{aligned}\left\langle \Omega^p_1, \Omega^n_2 \middle| V_{pn} \middle| \Omega^p_1, \Omega^n_2 \right\rangle = \sum_{j_1, j_2, j'_1, j'_2, J} & C^{\Omega_1}_{j_1} C^{\Omega_2}_{j_2} \\ & \times \langle j_1 \Omega_1,\, j_2 \Omega_2 | J\, \Omega_1 + \Omega_2 \rangle C^{\Omega_1}_{j'_1} C^{\Omega_2}_{j'_2} \\ & \times \langle j'_1 \Omega_1,\, j'_2 \Omega_2 | J\, \Omega_1 + \Omega_2 \rangle \\ & \times \left\langle j^p_1\, j^n_2,\, J \middle| V_{pn} \middle| j'^{\,p}_1\, j'^{\,n}_2,\, J \right\rangle. \end{aligned} \tag{2}$$

*Electronic address: sgyks@istanbul.edu.tr

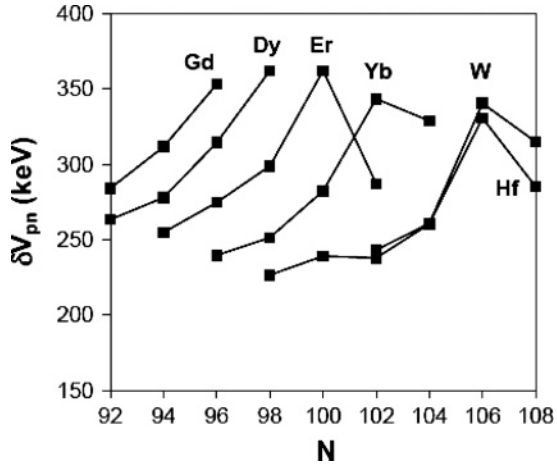

FIG. 1. Empirical δV_{pn} values for nuclei from Gd to W for N between 92 and 108. The p-n interactions are attractive, but, for visual convenience, the δV_{pn} values are plotted as positive. Extracted from Ref. [8].

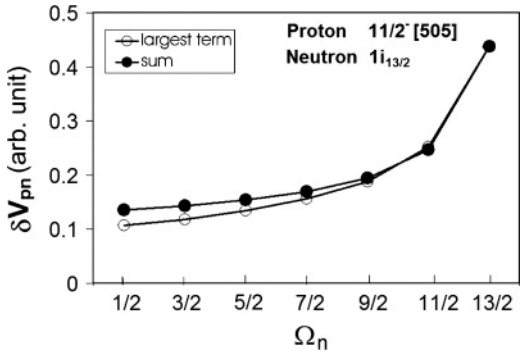

FIG. 2. Calculation of the interactions of a proton in the unique parity $\frac{11}{2}^-[505]$ orbit with neutrons in the unique parity orbits $\frac{1}{2}^+[660]\ldots\frac{13}{2}^+[606]$. In each case the largest term, by far, is the diagonal one (open circles). The sum in Eq. (2) is given by the filled circles.

The three expressions for the other $\Omega^{\rm tot}$ terms are similar, differing primarily in phase factors. These phase factors arise both in the Clebsch-Gordan coefficients, when Ω values change sign, and in the C_j coefficients, where one has $C_j^{-\Omega} = C_j^{\Omega}\,(-1)^{j-1/2+\ell}$. Note that the sums extend not only over the C_j coefficients (the j_p, j_n values), but also over the total angular momenta J to which they can couple. Note also that, in general, the interaction matrix elements also depend on J. Owing to the different total Ω values, the four cases differ in the ranges of J values summed over. Nevertheless, the four $\Omega^{\rm tot}$ values give identical results, and therefore the total p-n matrix element is just four times that in Eq. (2).

Any particular interaction can be substituted for V_{pn} in Eq. (2). Here, for simplicity we use a zero-range δ_{pn} interaction including spin exchange. The matrix elements in a spherical single-particle basis have been calculated and provided to us by A. De Maesschalck [11].

It is instructive to understand these interactions physically and intuitively with a simple first test case. Consider the interaction of a proton in the unique parity $\frac{11}{2}^-[505]$ orbit with a neutron in the seven orbits stemming from the $1i_{13/2}$ shell, namely, $\frac{1}{2}^+[660]$, $\frac{3}{2}^+[651]\ldots\frac{13}{2}^+[606]$. The orbital plane of the proton orbit is perpendicular to the symmetry axis of a prolate rotor, while the neutron orbits vary from nearly perpendicular to nearly parallel to this plane in going from $\frac{1}{2}^+[660]$ to $\frac{13}{2}^+[606]$. Therefore the interaction strength should grow as the neutron Ω_n value increases from $\frac{1}{2}$ to $\frac{13}{2}$. The results are shown in Fig. 2. Given the simple Nilsson wave functions for these unique parity orbits, specified by $C^p_{j=11/2} = 1$ ($\frac{11}{2}^-[505]$ Nilsson orbit), $C^n_{j=13/2} \sim 1$ ($\frac{1}{2}^+[660]$, $\frac{3}{2}^+[651]\ldots$, $\frac{11}{2}^+[615]$), and $C^n_{j=13/2} = 1$ ($\frac{13}{2}^+[606]$), it is

Z\N	92	94	96	98	100	102	104	106	108
$_{64}$Gd	p 5/2[413] n 3/2[521]	p 5/2[413] n 3/2[521]	p 5/2[413] n 3/2[521]						
$_{66}$Dy	p 3/2[411] n 3/2[521]	p 3/2[411] n 3/2[521]	p 3/2[411] n 5/2[642]	p 3/2[411] n 5/2[523]					
$_{68}$Er		p 7/2[523] n 3/2[521]	p 7/2[523] n 5/2[523]	p 7/2[523] n 5/2[523]	p 7/2[523] n 7/2[633]	p 7/2[523] n 1/2[521]			
$_{70}$Yb			p 1/2[411] n 5/2[523]	p 1/2[411] n 5/2[523]	p 1/2[411] n 7/2[633]	p 1/2[411] n 1/2[521]	p 1/2[411] n 5/2[512]		
$_{72}$Hf				p 7/2[404] n 5/2[523]	p 7/2[404] n 7/2[633]	p 7/2[404] n 1/2[521]	p 7/2[404] n 5/2[512]	p 7/2[404] n 7/2[514]	p 7/2[404] n 9/2[624]
$_{74}$W						p 7/2[404] n 1/2[521]	p 7/2[404] n 1/2[521]	p 7/2[404] n 7/2[514]	p 7/2[404] n 9/2[624]

FIG. 3. Ground state proton (upper) and neutron (lower) Nilsson orbits occupied by the last proton and neutron for the nuclei in Fig. 1, taken from the Nilsson assignments to the ground states of the neighboring A-1 odd-A nuclei.

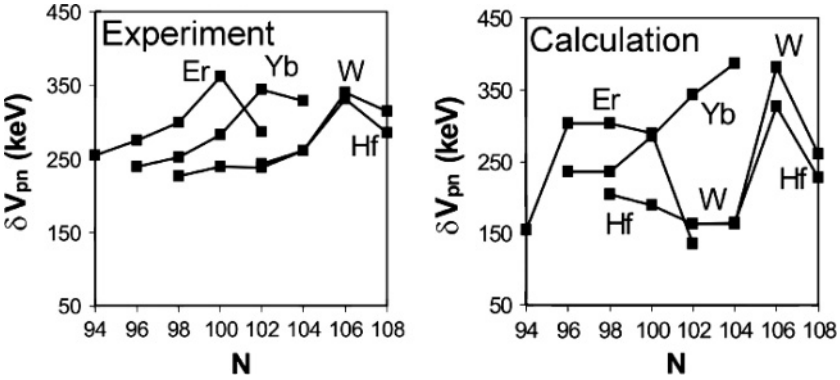

FIG. 4. Left, data on δV_{pn} from Fig. 1 for Er-W. Right, calculated values of the *p-n* interaction with a zero-range δ force between the last occupied proton and neutron orbits. The results are normalized to ^{172}Yb.

hardly surprising that the diagonal terms $\langle 1h^p_{\frac{11}{2}}, 1i^n_{\frac{13}{2}}, J|V_{pn}|1h^p_{\frac{11}{2}}, 1i^n_{\frac{13}{2}}, J\rangle$ completely dominate.

The behavior is exactly as expected. The strongest interaction, by far, of the proton in the $\frac{11}{2}^-$[505] orbit is with the $\frac{13}{2}^+$[606] orbit, and the weakest is with the $\frac{1}{2}^+$[660] orbit. There is a smooth and accelerating increase in the interaction as the neutron orbits change from Ω-$\frac{1}{2}$ to $\frac{13}{2}$.

To proceed with realistic calculations (within our simplified model) for the nuclei in Fig. 1, we first give, in Fig. 3, the ground state proton and neutron orbits for these nuclei obtained from the level schemes of the neighboring odd-*A* nuclei. Then, using Eq. (2) we calculate the δ_{pn}-function interactions. Given the simplicity of the present approach, no serious attempt was made to include pairing correlations. However, as a step in this direction, in those cases where an excited Nilsson orbit was found in the neighboring odd *Z* or *N* nucleus at an excitation energy <80 keV, the interactions for that orbit and the ground state orbit were averaged. This affects only a few calculated δV_{pn} values by about 50 keV and a few others by amounts of ∼10 keV. The results are shown in Figs. 4 and 5.

Overall, despite their extreme simplicity (zero-range δ_{pn} interaction, virtually no pairing correlations taken into account, assumption of constant deformation), the calculations reproduce the data rather well. For the heavier isotopes (Er–W), the calculations (see Fig. 4) exhibit an upward slope similar to the empirical δV_{pn} values. For those cases where the data extend to large enough neutron numbers, they even reproduce the dropoff in δV_{pn}. The only important discrepancies are that the calculated δV_{pn} values peak for Er a little early and that there is no falloff for Yb with $N = 104$. In contrast, the calculations for Gd and Dy are only in fair agreement with the data, although the overall magnitude is about right (See Fig. 5). At least in the case of Gd, it is clear why the calculated δV_{pn} values are constant: from Fig. 3, we see that exactly the same orbits are occupied for the three successive isotopes with $N = 92$, 94, and 96.

The reason that this occurs, of course, is the crossing of Nilsson orbits as the deformation grows in these transitional nuclei. For Gd, we have also calculated δV_{pn} for $N = 98$ even though the orbit for the last proton is not known experimentally. However, the existing data for the Eu isotopes show that the ground state proton orbit, $\frac{5}{2}^+$[413], is rather stable. Moreover, calculations [12] suggest that that orbit likely remains the ground state for larger neutron numbers. Making the assumption that this continues for $N = 98$, we see, interestingly, that the calculations do show a sharp rise (for N = 98), albeit delayed relative to the data.

To summarize, empirical *p-n* interactions of the last proton with the last neutron show a remarkably simple and regular pattern of parallel tracks against neutron number. A simple explanation, in which the neutrons in specific Nilsson orbits have increasingly higher overlaps with mid-shell proton orbits as *N* increases from 92 toward the mid-neutron shell, is tested by calculations of the *p-n* interaction matrix elements, using a zero-range δ interaction and transforming the matrix element into a spherical single-particle basis. Good overall agreement, in a constant deformation model, is obtained for Er, Yb, Hf, and W. For Gd and Dy the calculations give the right general

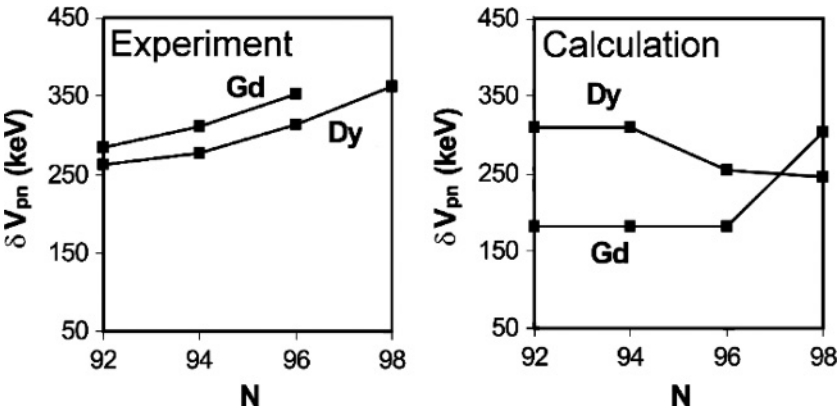

FIG. 5. Left, Data on δV_{pn} from Fig. 1 for Gd and Dy. Right, Calculated values. The results are normalized to the value for ^{172}Yb in Fig. 4.

magnitude (recall that there is only one normalization for all the nuclei in Figs. 4 and 5), but the detailed trends in the data are not reproduced. It would be interesting to measure δV_{pn} for ^{162}Gd (only the mass of ^{160}Sm is needed for this) to see whether the empirical value does increase as in the calculations.

Of course, with such a simple approach, one would not expect better agreement than we have obtained. It would be very interesting to see if rigorous, self-consistent calculations with realistic interactions can reproduce the data more accurately while still capturing essentially the same underlying physics interpretation. Work along such lines is in progress [13].

We are deeply grateful to K. Heyde for extensive discussions, for much guidance throughout this project, and for help in understanding issues involved in calculating these p-n interactions in the spherical single-particle basis. We thank A. de Maesschalck for providing the δ-function matrix elements in a single-particle basis. Work supported by U.S. Departments of Energy grants DE-FG02-91ER40609 and DE-FG02-88ER40417.

[1] J.-Y. Zhang *et al*., in *Contemporary Topics in Nuclear Structure Physics, Cocoyoc, Mexico, 1988, Book of Abstracts*, p. 109.
[2] J.-Y. Zhang, R. F. Casten, and D. S. Brenner, Phys. Lett. **B227**, 1 (1989).
[3] D. S. Brenner, C. Wesselborg, R. F. Casten, D. D. Warner, and J.-Y. Zhang, Phys. Lett. **B243**, 1 (1990).
[4] P. Van Isacker, D. D. Warner, and D. S. Brenner, Phys. Rev. Lett. **74**, 4607 (1995).
[5] G. Audi, A. H. Wapstra, and C. Thibault, Nucl. Phys. **A729**, 337 (2003).
[6] R. B. Cakirli, D. S. Brenner, R. F. Casten, and E. A. Millman, Phys. Rev. Lett. **94**, 092501 (2005).
[7] R. B. Cakirli and R. F. Casten, Phys. Rev. Lett. **96**, 132501 (2006).
[8] D. S. Brenner, R. B. Cakirli, and R. F. Casten, Phys. Rev. C **73**, 034315 (2006).
[9] K. Heyde, P. Van Isacker, R. F. Casten, and J. L. Wood, Phys. Lett. **B155**, 303 (1985).
[10] B. Nilsson, Nucl. Phys. **A129**, 445 (1969).
[11] A. De Maesschalck (private communication).
[12] W. Nazarewicz, M. A. Riley, and J. D. Garrett, Nucl. Phys. **A512**, 61 (1990).
[13] M. Stoitsov and W. Nazarewicz (private communication).